Natural Toxins
Nat. Toxins **6**: 219–233 (1998)

RESEARCH ARTICLE

Fine Structural Changes in the Ileum of Mice Fed on δ Endotoxin-Treated Potatoes and Transgenic Potatoes

Nagui H. Fares*[1] and Adel K. El-Sayed[2]
[1]Department of Zoology, Faculty of Science, Ain Shams University, Cairo, Egypt
[2]Department of Entomology, Faculty of Science, Ain Shams University, Cairo, Egypt

ABSTRACT The present work has been designed to study the effect of feeding on transgenic potatoes, which carry the CryI gene of *Bacillus thuringiensis* var. *kurstaki* strain HD1, on the light and electron microscopic structure of the mice ileum, in comparison with feeding on potatoes treated with the 'δ-endotoxin' isolated from the same bacterial strain. The microscopic architecture of the enterocytes of the ileum of both groups of mice revealed certain common features such as the appearance of mitochondria with signs of degeneration and disrupted short microvilli at the luminal surface. However, in the group of mice fed on the 'δ-endotoxin', several villi appeared with an abnormally large number of enterocytes (151.8 in control group versus 197 and 155.8 in endotoxin and transgenic-treated groups, respectively). Fifty percent of these cells were hypertrophied and multinucleated. The mean area of enterocyte was significantly increased (105.3 μm^2 in control group versus 165.4 μm^2 and 116.5 μm^2 in endotoxin and transgenic-treated groups, respectively). Several forms of secondary lysosomes or auotophagic vacuoles were recognized in these cells. These changes were confirmed with the scanning electron microscope which revealed a remarkable increase in the topographic contour of enterocytes (23 μm in control group versus 44 μm and 28 μm in endotoxin and transgenic-treated groups, respectively) at the divulged surface of the villi. The basal lamina along the base of the enterocytes was damaged at several foci. Several disrupted microvilli appeared in association with variable-shaped cytoplasmic fragments. Some of these fragments contained endoplasmic reticulum, as well as ring-shaped annulate lamellae. In addition, the Paneth cells were highly activated and contained a large number of secretory granules. These changes may suggest that δ-endotoxin-treated potatoes resulted in the development of hyperplastic cells in the mice ileum. Although mild changes are reported in the structural configuration of the ileum of mice fed on transgenic potatoes, nevertheless, thorough tests of these new types of genetically engineered crops must be made to avoid the risks before marketing. Copyright © 1998 John Wiley & Sons, Ltd.

Key words: scanning; ultrastructure; ileum; *Bacillus thuringiensis* var. *kurstaki*; transgenic potatoes; δ-endotoxin

INTRODUCTION

This study respects the efforts of several investigators against the dangerous use of chemical insecticides for pest control; these chemicals are still widely marketed (Fares, 1996). In the mid 1970s, the World Health Organization (WHO) and other international institutions initiated studies on the development of existing and new biological control agents (de Barjac, 1989). The most popular of these agents are strains of the '*Bacillus thuringiensis*'. Among these *Bacillus thuringiensis* var. *kurstaki*, was proven to produce an effective toxin against lepidopteran insects (Tyrell *et al.*, 1981, de Barjac, 1989; Singsit *et al.*, 1997). These spore-forming entomopathogenic bacteria are gram-positive and have a unique ability to produce parasporal-proteinaceous crystalline inclusions during sporulation (Caramori *et al.*, 1991; Sanchis *et al.*, 1996). The insecticidal properties of this protein crystal (δ-endotoxin) have stimulated studies leading to its commercial production for use as a biological control agent (Sanchis *et al.*, 1996). Scientists at AGERI

*Correspondence to: Dr N. H. Fares, Department of Zoology, Faculty of Science, Ain Shams University, Cairo, Egypt.
E-mail: nfares@asunet.shams.eun.eg
Sponsors: This work is partially supported by a Fullbright Post-doctoral Scholarship to Nagui Hassan Fares.

Received 6 October 1998; Accepted 13 January 1999.

CCC 1056–9014/98/060219–15 $17.50

Figure 1. Scanning electron micrograph of the intestinal mucosa of control group revealing the luminal surface of the villi covered by enterocytes (E) and occasional small pits indicating the sites of mucous cells (m). Bar = 10 μm

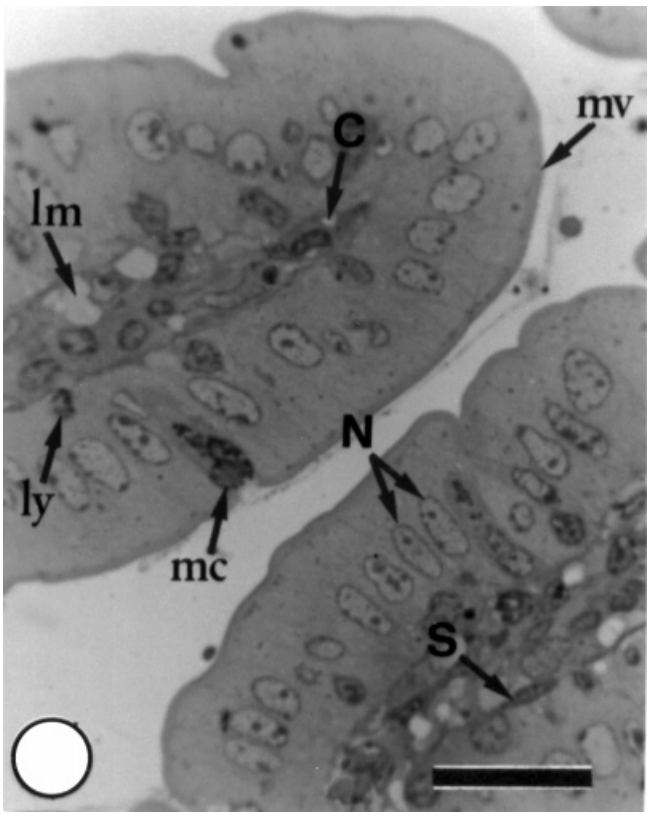

Figure 2. Semithin section of the intestinal villi of the control group revealing the enterocytes with typical oval nuclei (N) and a continuous thin ribbon of tightly packed microvilli (mv), mucous cells (mc), with their dark mucin granules, intraepithelial lymphocytes (ly), blood capillaries (C), lymphatics (lm) and smooth muscles (S). Bar = 20 μm

(Agriculture Genetic Engineering Research Institute, Guiza, Egypt) were able to produce transgenic potatoes in which the CryI gene of *Bacillus thuringiensis* var. *kurstaki* was transmitted into the plant cells via a shuttle plasmid vector after cloning in *E. coli*. The present investigation has been designed to evaluate feeding of experimental animals on 'transgenic potatoes' (as yet not measured) on the ileum of mice at the microscopic level, compared with feeding on potatoes treated with the bacterial toxin 'δ-endotoxin'.

MATERIALS AND METHODS

Preparation of Bacterial Endotoxin

Bacterial isolates of the strain HD14 of *Bacillus thuringiensis* var. *kurstaki* were allowed to grow in sterilized T3 medium (5.0 g peptone, 1.5 g yeast extract, 0.005 g Mn Cl_2 and 0.5 M sodium phosphate buffer at pH 6.8) according to Travers *et al.* (1987). Sporulation was examined at intervals using a light microscope. Bacterial spores and crystals were collected using a Backman J-2MC centrifuge equipped with a JA-14 titanium rotator at 1200 rev min^{-1} for 20 min at 4 °C. Sedimented spores and crystals (δ-endotoxin) were washed in distilled water and dried for 6 h (under vacuum) in 'Labconco, Freeze Dry/Shell Freeze' system (model ilyph, lock 6) according

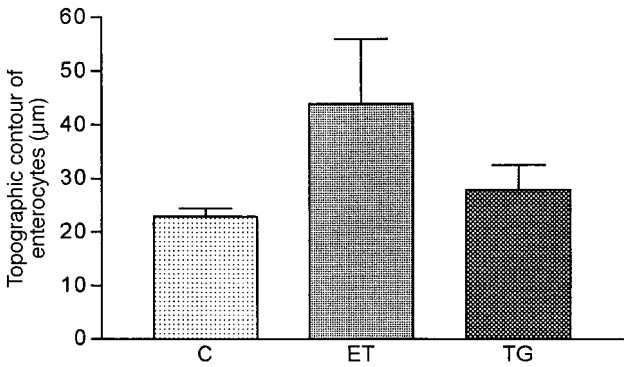

Figure 3. Variation in the topographic control of enterocytes in in SEM images of ileum for each of the three groups of mice: control group (C), δ-endotoxin-treated group (ET) and transgenic potatoes-treated group (TG). Bars denote the standard deviation in each group

Table 1. Statistical analysis of the mean perimeter (topographic contour) of enterocyte in scanning electron microscopic images of ileum for each of the three different groups of mice: control group (C), δ-endotoxin-treated group (ET), and transgenic potatoes-treated group (TG)

	Control (C)	Endotoxin (ET)	Transgenic (TG)
Number of measured cells	50	50	50
Mean perimeter of cell in 5 mice	**23.00**	**44.00**	**28.00**
Minimum perimeter of cell	21.00	30.00	22.00
Median perimeter of cell	24.00	44.00	30.00
Maximum perimeter of cell	24.00	58.00	32.00
Standard deviation	1.477	11.94	4.513
Standard error	0.4264	3.447	1.303
p value (two-tailed)	$p < 0.0001$	$p < 0.0001$	$p < 0.0001$
Significant (alpha = 0.05)?	Yes	Yes	Yes
Unpaired *t*-test:	Two-tailed p value:		
1: C vs ET	p value <0.0001 (means are significantly different, $p < 0.05$)		
2: C vs TG	p value = 0.0014 (means are significantly different, $p < 0.05$)		

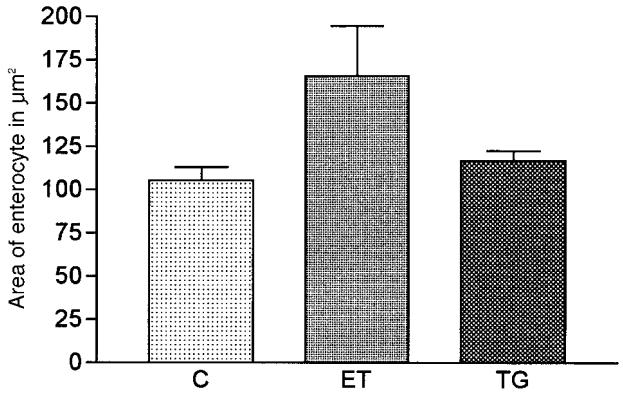

Figure 4. Variation in the area of enserocytes in semithin sections of ileum of each of the three different groups of mice: control group (C), δ-endotoxin-treated group (ET) and transgenic potatoes-treated group (TG). Bars denote the standard deviation in each group

to Redway and Lapage (1974). The dried δ-endotoxin was stored at 20 °C. Fresh potatoes were cut into small pieces and immersed in a suspension of the δ-endotoxin, of *Bacillus thuringiensis* var. *kurstaki*, in distilled water (1 g l^{-1}) for 30 min.

Feeding of Mice

A group of 5 1-month-old male mice (*Mus musculus*), was fed daily for 2 weeks on a diet consisting of the δ-endotoxin-treated potatoes. Another group of 5 mice was fed on a diet consisting of transgenic potatoes, carrying the CryI gene of *Bacillus thuringiensis* var. *kurstaki*, for 2 weeks. These transgenic plants were provided by AGERI (Guiza, Egypt). A control group of 5 mice was fed on fresh potatoes for the same 2-week period.

Table 2. Statistical analysis of the mean area of enterocyte in semithin sections of ileum of each of the three different groups of mice. control group (C), δ-endotoxin-treated group (ET), and transgenic potatoes-treated group (TG)

	Control (C)	Endotoxin (ET)	Transgenic (TG)
Number of measured cells	750	750	750
Mean area of cell in 5 mice	**105.3**	**165.4**	**116.5**
Minimum area of cell	99.00	125.0	111.0
Median area of cell	103.5	172.0	115.0
Maximum area of cell	115.0	192.5	125.0
Standard deviation	7.762	28.70	5.972
Standard error	3.881	14.35	2.986
p value (two tailed)	$p < 0.0001$	$p < 0.0014$	$p < 0.0001$
Significant (alpha = 0.05)?	Yes	Yes	Yes
Unpaired *t*-test:	Two-tailed p value:		
1: C vs ET	p value = 0.0068 (means are significantly different, $p < 0.05$)		
2: C vs TG	p value = 0.06 (means are not significantly different, $p < 0.05$)		

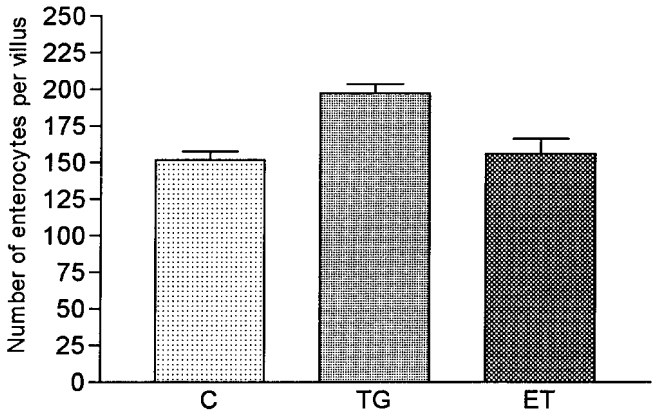

Figure 5. Variation in number of enterocytes pervillus in semithin sections of ileum of each of the three different groups of mice: control group (C), δ-endotoxin-treated group (ET) and transgenic potatoes-treated group (TG), Bars denote the standard deviation in each group

Table 3. Statistical analysis of the mean number of enterocytes in semithin sections of ileum of each of the three different groups of mice: control group (C), δ-endotoxin-treated group (ET), and transgenic potatoes-treated group (TG)

	Control (C)	Endotoxin (ET)	Transgenic (TG)
Number of villi selected in 5 mice	625	625	625
Mean number of cells per villus (in 5 mice)	**151.8**	**197.0**	**155.8**
Minimum number of cells	148.0	190.0	140.0
Median number of cells	149.5	196.5	160.5
Maximum number of cells	160.0	205.0	162.0
Standard deviation	5.560	6.164	10.53
Standard error	2.780	3.082	5.266
p value (two tailed)	$p < 0.0001$	$p < 0.0001$	$p < 0.0001$
Significant (alpha = 0.05)?	Yes	Yes	Yes
Unpaired t-test:	Two-tailed p value:		
1: C vs ET	p value < 0.0001 (means are significantly different, $p < 0.05$)		
2: C vs TG	p value = 0.5268 (means are not significantly different, $p < 0.05$)		

Preparation of Microscopic Samples

Animals from the three different groups were killed by severing the spinal cord and the ileum of each animal was dissected out, cut into small pieces and fixed in 2.5 % glutaraldehyde in 0.l M phosphate buffer (Sigma, St Louis, USA) at pH 7.2 for 90 min, for light, scanning and electron microscopic studies. Tissues were postfixed for 2 h in 1 % OsO^4 in the same phosphate buffer, dehydrated through ascending grades of acetone and embedded in Spurr's medium. Semithin sections (0.5 μm) were prepared on an MT600-XL RMC ultratome (Tokyo, Japan), stained with toluidine blue and used for light microscopic studies. Thin sections (80–90 nm) were cut with a Diatom diamond knife (Washington, USA) on an MT600-XL RMC ultratome (Tokyo, Japan). Sections were collected on 200-mesh nickel grids, stained in 5% uranyl acetate in distilled water for 10 min, washed in distilled water and stained in lead citrate for 6 min (Venable and Coggeshall, 1965) and examined with a bi-functional Joel JTM-1200 EX II electron microscope (Tokyo, Japan). For scanning electron microscopic studies, small pieces of the OsO_4-postfixed tissues were exposed to the critical point dry and spotter coating processes and examined by the same electron microscope.

Morphometric Analysis

Semithin sections, as well as scanning and electron microscopic photographs, of the ileum of each of the three different groups of mice were used in the morphometric studies. Images of the ileum from these preparations were transferred into an IBM computer

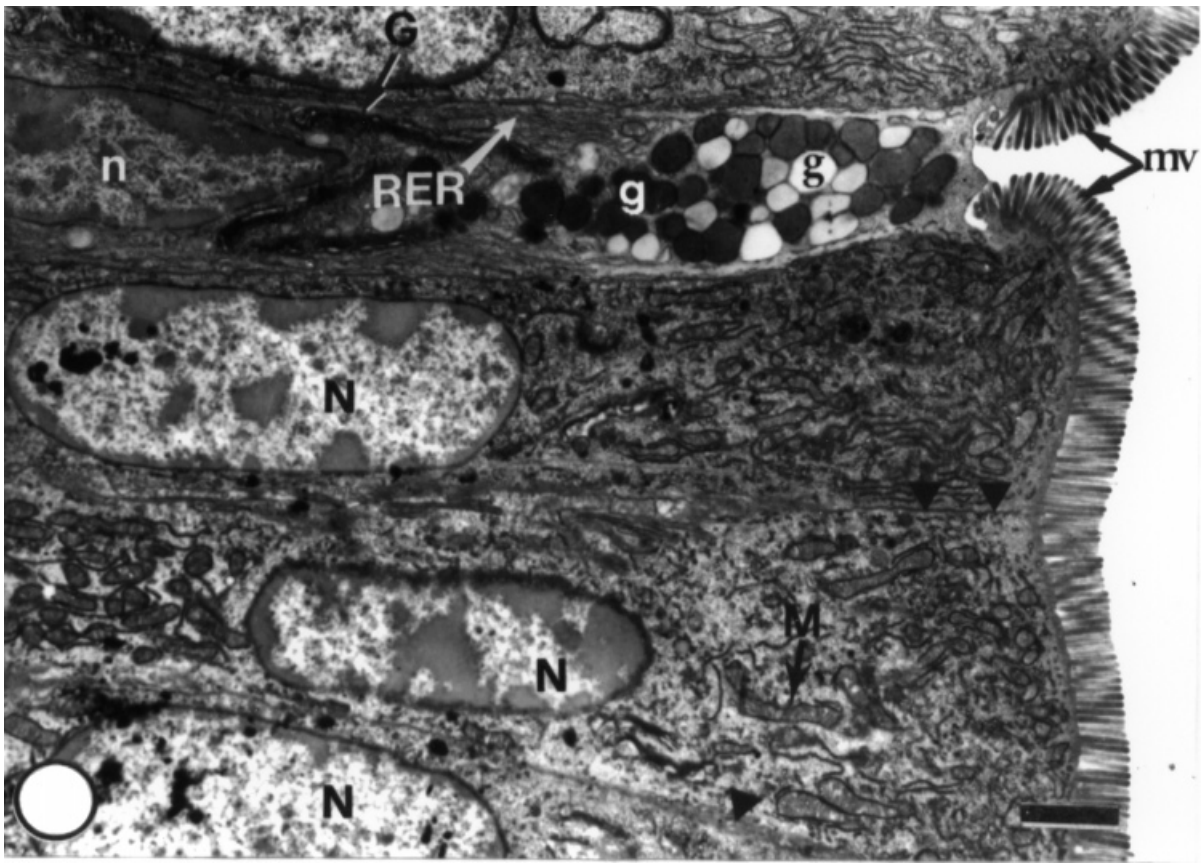

Figure 6. Electron micrograph of the intestinal epithelium of control group revealing a mucous cell with apical mucin globules (g), basal flattened nucleus (n), rough endoplasmic reticulum (RER) and Golgi complex (G). The enterocytes display luminal microvilli (mv), large oval euchromatic nuclei (N), tight junction (arrows), rough endoplasmic reticulum (arrow heads) and mitochondria (M). Bar = 2.0 μm

attached to an Olympus™ light microscope (Japan) via a Sony™ video-camera (Japan). The captured images were then digitized on the computer using an 'Alpha-Viewer' image analysis program, version 1.0, for measuring the topographic contour and the area of enterocytes. The number of enterocytes, multinucleated enterocytes, and hypertrophied nuclei were also counted. The mean value of each parameter was calculated per 5 animals, in each of the three different groups, and the data were statistically analysed using Paired Student's *t*-test of the 'GraphPad Prism™' program, version 2.01, from GraphPad Software Inc., USA.

OBSERVATION
Microscopic Observations

In relation to the digestive and absorptive functions of the small intestine of mammals, the mucosa of the ileum is the most important absorptive layer (Fawcett, 1997). Accordingly, the present investigation was designed to focus mainly on the microscopic structure of this layer in mice of the three different groups: the control group, the group fed on the δ-endotoxin-treated potatoes and the group fed on transgenic potatoes.

Control Group

As revealed by the scanning electron microscopic examination, the intestinal mucosa was thrown up into several finger-like, as well as leaf-like forms of villi extending into the intestinal lumen (Figure 1). The surface of these villi was almost entirely covered by the enterocytes, which were the principle absorptive cells of the intestinal epithelium. The topographic contour (mean perimeter) of the enterocyte was 23 μm, $p < 0.0001$ (Table 1, Figure 3). Scattered among the enterocytes were occasional small pits indicating the sites of mucous cells. The light microscopic examination of semithin sections of these villi revealed the enterocyte as a tall columnar cell with typical oval nuclei in the lower third of the cell (Figure 2). The mean area of the enterocyte was 105.3 μm^2, $p < 0.0001$ (Table 2, Figure 4), while the mean number per one villus was 151.8, $p < 0.0001$

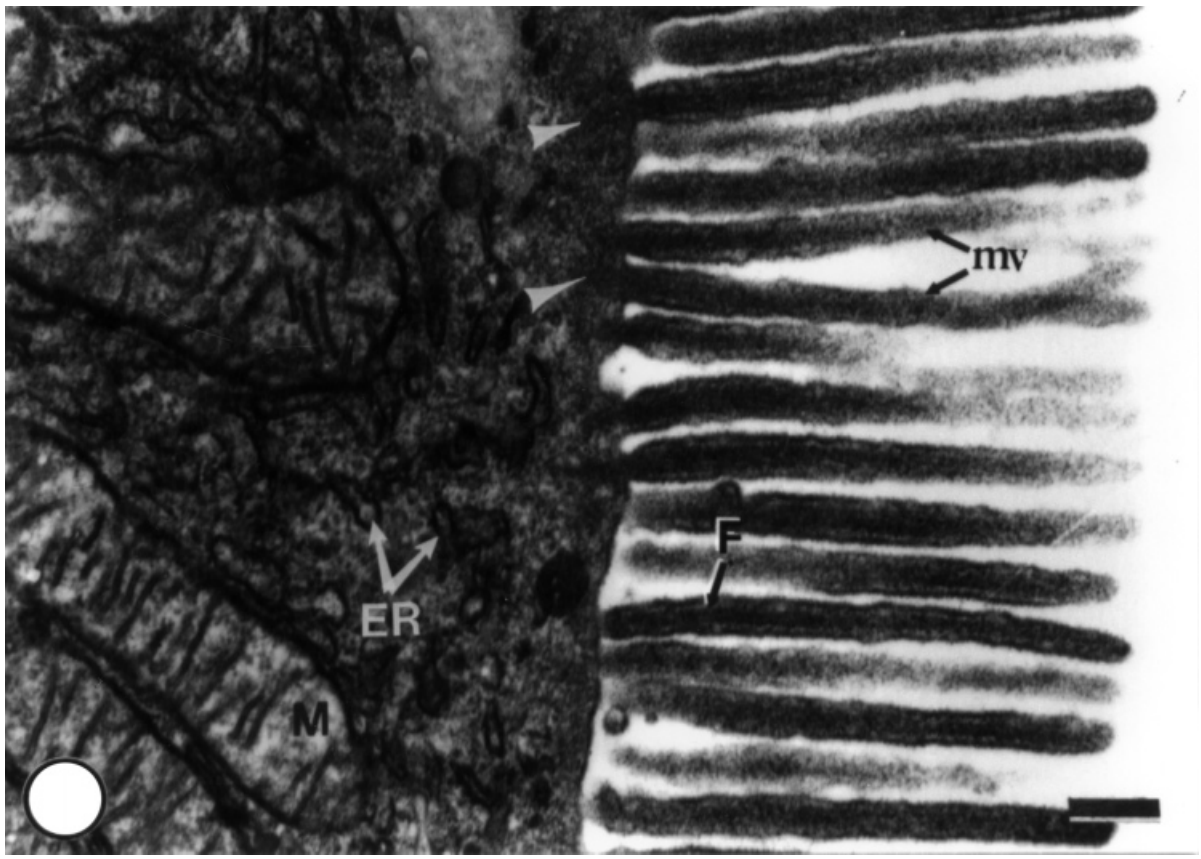

Figure 7. Electron micrograph of the intestinal epithelium of control group revealing a part of an enterocyte with relatively tall mitochondria (M), several profiles of endoplasmic reticulum (ER) and a large numbers of closely packed parallel microvilli (mv). Each microvillus has a bundle of thin striated filaments (F) connected to terminal web (arrow heads) in a clear zone of underlying cytoplasm. Bar = 0.2 μm

(Table 3, Figure 5). The luminal surface of these cells was covered by a continuous thin ribbon, which was a highly specialized region of this epithelium, consisting of tightly packed microvilli. Mucous cells were located among the enterocytes and were distinguished by their mucin granules which occupy the upper portion of the cells. Their nuclei were small in size and oval in shape and were located at the basal side of the cells. Intraepithelial lymphocytes were located in a basal position between the lateral intercellular spaces. They possessed relatively small dark nuclei. Underneath the basal lamina of the intestinal epithelium, the lamina propria penetrated the core of the villi, taking along blood capillaries, lymphatics and smooth muscles.

At the ultrastructural level, the mucous cells were recognized by their mucin globules (Figure 6). These droplets occupied the apical region of the cell and consisted of a homogeneous matrix, which varied in intensity from highly electron dense to more lightly electron dense, enveloped by a delicate membrane. The base of the cell was relatively free of secretory material and formed a slender stem or stalk. The nucleus tended to be flattened and was surrounded by a thin layer of cytoplasm. This cytoplasmic area contained several profiles of longitudinally oriented rough endoplasmic reticulum running parallel to the lateral edges of the cell. A highly developed Golgi complex was situated between the nucleus and the mucin droplets.

The enterocytes displayed large oval euchromatic nuclei with a few patches of heterochromatin (Figure 6). The lateral walls of these cells formed a well-developed tight junction, specially at the uppermost region. The upper cytoplasmic region was rich in rough endoplasmic reticulum and mitochondria.

The mitochondria were relatively large and had an internal structure with several large cristae traversing across the inner mitochondrial space (Figure 7). The striated or brush border of the enterocytes was made up of large numbers of closely packed parallel microvilli (Figures 6 and 7). Each microvillus was a cylindrical protrusion of the apical cytoplasm and consisted of a cell membrane enclosing a filamentous core. In the interior of

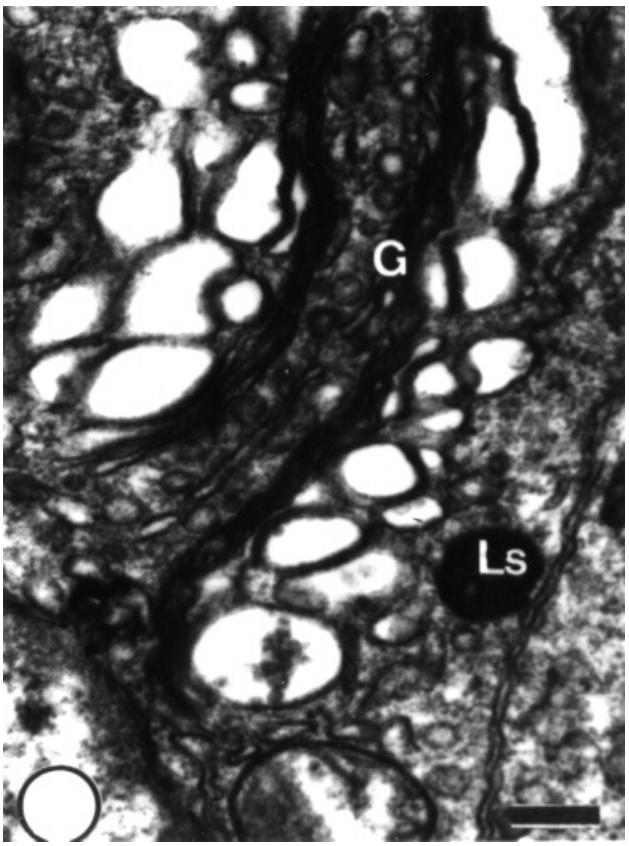

Figure 8. Electron micrograph of the intestinal epithelium of control group revealing a part of an enterocyte with well-developed Golgi apparatus (G) and a primary lysosome (Ls). Bar = 0.2 μm

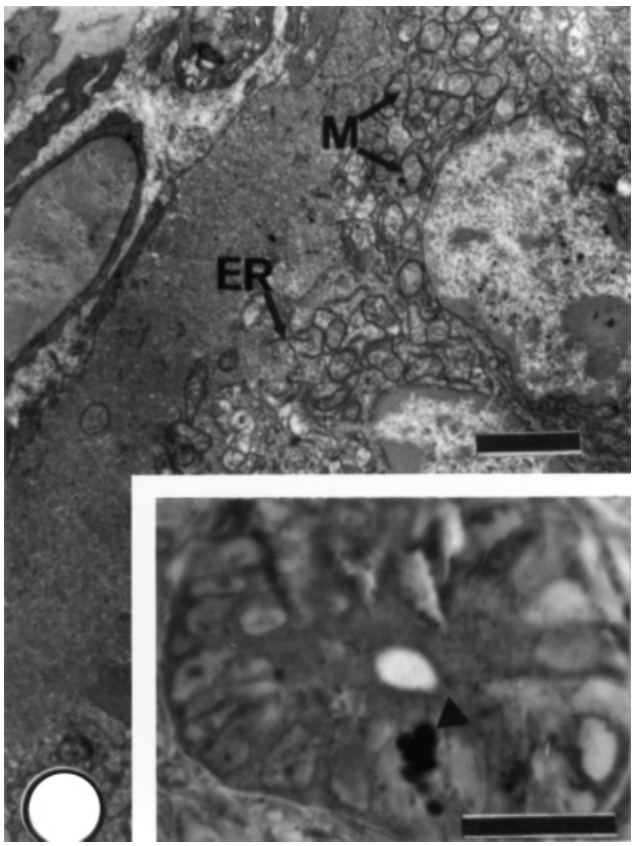

Figure 9. Electron micrograph of a basal region of intestinal epithelium of a control mouse revealing a large number of subnuclear mitochondria (M), a few profiles of endoplasmic reticulum (ER) and a thick basal lamina (asterisk). Bar = 2.0 μm. The inset reveals a semithin section of a part of the crypt of Lieberkühn containing a few Paneth cells with dark secretory granules (arrowhead). Bar = 20 μm

each microvillus was a bundle of thin striated filaments of running longitudinally in an otherwise homogeneous fine-textured cytoplasmic matrix (Figure 7). Underneath the microvilli was a clear zone usually devoid of organelles, except for a few profiles of endoplasmic reticulum, but occupied by filamentous striations, or terminal web, parallel to the apical surface of the cell (Figure 7).

Several well-developed Golgi apparatuses occupied a supranuclear position and consisted of parallel cisternae and large vesicles (Figure 8). A few primary lysosomes were located in the area of Golgi apparatus (Figure 8). The subnuclear cytoplasmic area was occupied by a large number of mitochondria and a few profiles of endoplasmic reticulum (Figure 9). The base of the enterocytes was based on a thick basal lamina (Figure 9). A small number of Paneth cells were recognized in the lower third of the crypts of Lieberkühn by their characteristic basal nuclei and secretory granules in their luminal surface (inset, Figure 9).

δ-Endotoxin-Treated Group

In the group of mice fed on the δ-endotoxin-treated potatoes, the scanning electron microscopic examination revealed a remarkable increase in the topographic contour of the enterocytes at the divulged surface of the villi (Figure 10). The mean perimeter of the enterocyte was 44 μm, $p < 0.0001$ (Table 1, Figure 2). In addition, several variable-shaped structures, ranging from round to elongate, were recognized adhering to these villi. In semithin sections, the villi appeared with an abnormally large number of enterocytes and consequently were extremely large (Figure 11). The mean number of enterocytes per villus was 197, $p < 0.0001$ (Table 3, Figure 5), while the mean area of enterocytes was 165.4 μm^2, $p < 0.0014$ (Table 2, Figure 4). A large number (50 %) of the enterocytes in these villi were multinucleated. The great majority of these nuclei were hypertrophied and acquired a round shape, rather than the oval appearance revealed in the enterocytes of the control group. At the ultrastructural level, the nuclei of the enterocytes displayed a typical rounded configuration

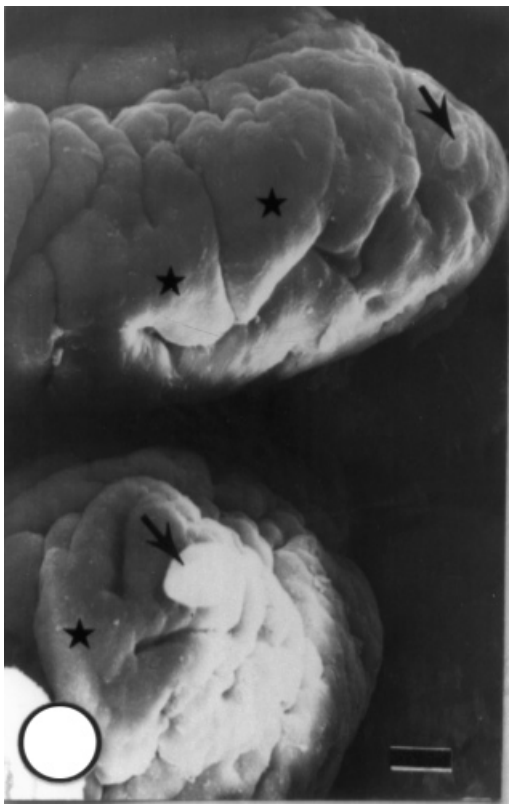

Figure 10. Scanning electron micrograph of the intestinal mucosa of δ-endotoxin-treated group revealing remarkably increased topographic contour of enterocytes (asterisks) and associated variable-shaped structures (arrows). Bar = 10μm

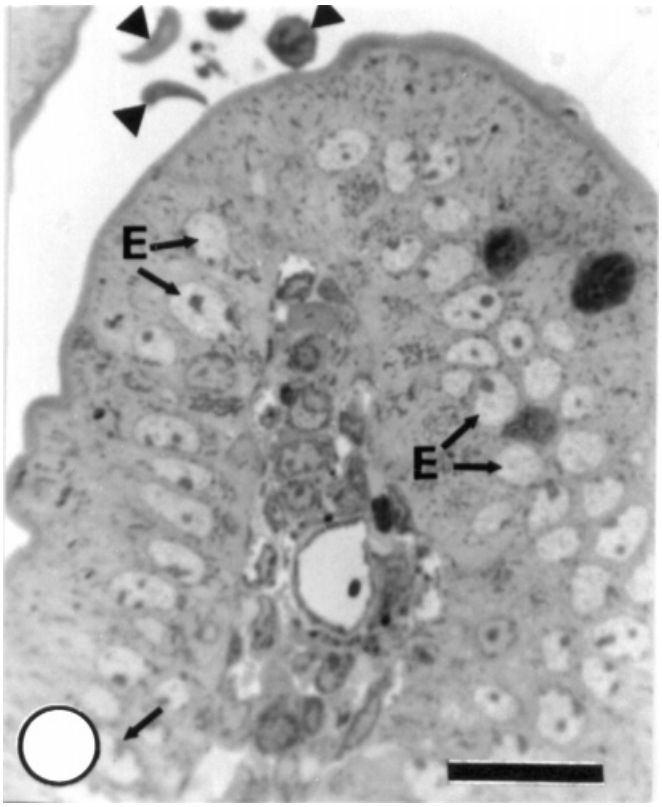

Figure 11. Semithin section of the intestinal mucosa of δ-endotoxin-treated group revealing a villus with an abnormally large number of multinucleated and hypertrophied enterocytes (E). A number variable-shaped cytoplasmic fragments (arrowheads) are in association with this villus. Bar = 20 μm

(Figures 11 and 12). In addition, the basal lamina along the base of the enterocytes was severely destructive at several foci. A number of enterocytes lost their luminal microvilli and appeared in association with variable-shaped cytoplasmic fragments (Figure 12). The rounded forms of these fragments contained several unrecognizable membranous structures, while the elongated forms contained several profiles of endoplasmic reticulum, as well as ring-shaped annulate lamellae (Figures 12 and 13). At one side, these cytoplasmic fragments possessed clear zones which extended laterally into vermiform processes (Figure 13). Most of these cytoplasmic fragments were in association with much smaller rounded structures which were remarkable for their highly electron dense contour and lightly dense core. The lateral plasma membranes of the enterocytes were detached in a number of foci (Figure 14). Their supranuclear cytoplasmic area contained several profiles of endoplasmic reticulum, a few mitochondria and several forms of secondary lysosomes, or auotophagic vacuoles (Figures 14 and 15). Several degenerated mitochondria, as well as endoplasmic reticulum, were located within the autophagic vacuoles (Figure 15). The luminal surface of the enterocytes were covered by short microvilli. The mucous cells in these villi contained several coagulated mucin granules (Figure 16 and inset). In the crypts of Lieberkühn, the Paneth cells were highly activated and contained large number of secretory granules (Figure 17).

Transgenic Potatoes-treated Group

In the group of mice fed on transgenic potatoes, both scanning and light microscopic architecture of the intestinal villi and their cellular structures, including enterocytes, Paneth cells, and mucous cells were almost as normal as the control group (Figures 18–20). The mean perimeter of enterocyte was 28 μm ($p < 0.0001$, Table 1, Figure 2), with a mean area of 116.5 ($p < 0.0001$, Table 2, Figure 4) and a mean number of 155.8 enterocytes per villus ($p < 0.0001$, Table 3, Figure 5). However, at the ultrastructural level the enterocytes possessed several dilated mitochondria with short cristae (Figure 21). In addition, the luminal surface of certain foci possessed disrupted short microvilli. Nevertheless, in the great majority of the enterocytes the microvilli displayed

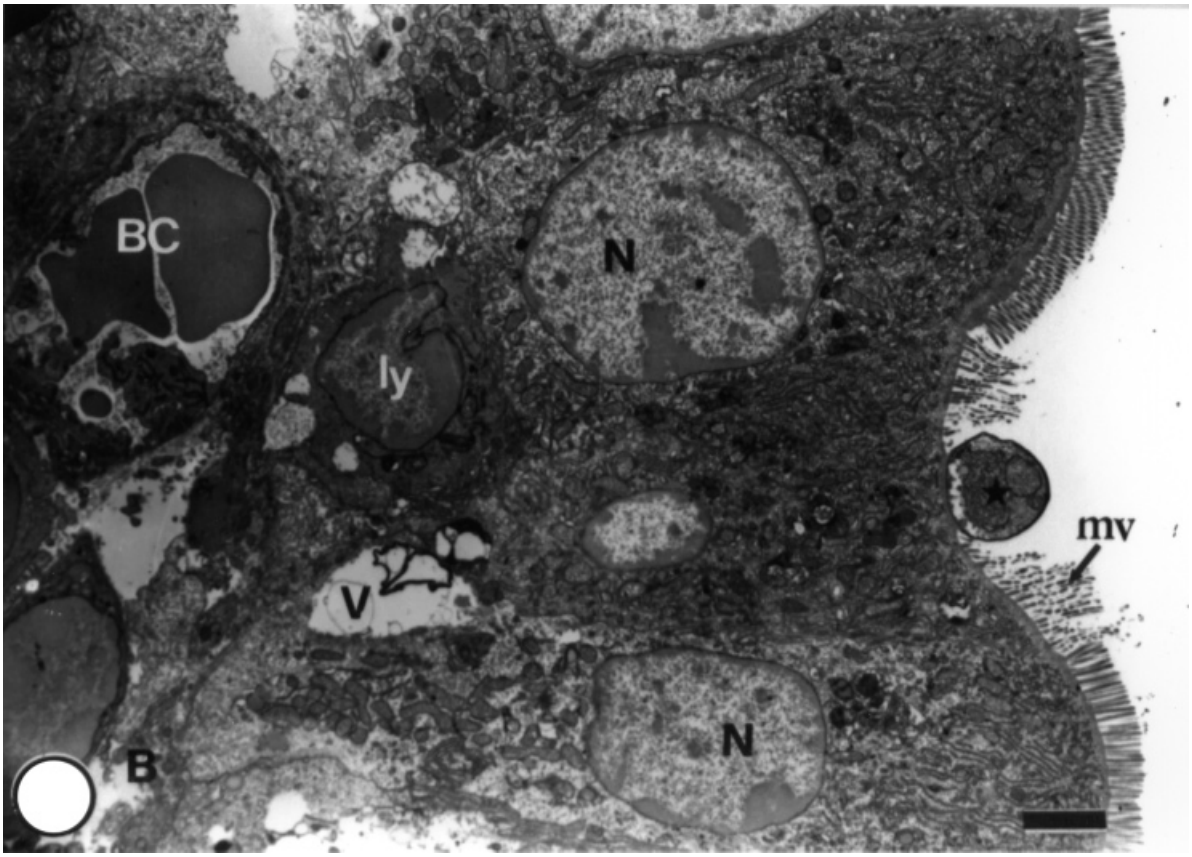

Figure 12. Electron micrograph of the intestinal mucosa of δ-endotoxin-treated group revealing enterocytes with rounded nuclei (N), intracellular vacuoles (V) and discontinuous basal lamina (B) interrupted by a lymphocyte (ly) and congested blood capillary (BC). A cytoplasmic fragment (asterisk) enclosing membranous structures is in association with fragmented microvilli (mv). Bar = 2.0 μm

regular striated appearance (Figure 22). The basal lamina was relatively intact (Figure 18). Mucous cells possessed a homogeneously electron dense mucin granules (Figure 20).

DISCUSSION

In the present investigation, the enterocytes of the intestinal epithelium in the group of mice fed on δ-endotoxin-treated potatoes were remarkably enlarged as a result of multiplication and hypertrophy of their nuclei, degeneration of mitochondria and endoplasmic reticulum, and the ensuing appearance of autophagic vacuoles. These features were reflected on the scanning topographic architecture of these cells, which showed a remarkably large contour. In addition, these changes were accompanied by the detachment of the lateral plasma membranes in several foci and the discontinuation of the basal lamina of these cells. Several investigations revealed that solubilized δ-endotoxin of *Bacillus thuringiensis kurstaki* is cytolytic to a wide range of vertebrate and invertebrate cells (Wu and Chang, 1985; Ibarra and Federici, 1986b; Chilcott and Ellar, 1988). Additionally, Thomas and Ellar (1983a) showed that solubilized endotoxin preparations are lethal when injected into suckling mice. It has been suggested that the high toxicity of this endotoxin is due not to a single protein, but rather to a set of nergistic interactions of the 25-kDa protein with one or more of the higher molecular weight proteins (Chilcott and Ellar, 1988). Although the precise mode of action of the δ-endotoxin of *Bacillus thuringiensis* var. *kurstaki* is not fully understood, Lüthy and Ebersold, (1981) suggested that intoxication in insects may result from an osmotic imbalance across the midgut epithelial membranes which leads quickly to hypertrophy and lysis of midgut cells. Lysis is followed by disruption of the basement membrane, leakage of digestive juices into the hemocoel, and larval death. Thomas and Eliar (1983b) provided good evidence that *Bacillus thuringiensis kurstaki* endotoxin's cytolytic activity was due to a detergent-like action in which the toxin disrupted membranes by binding to specific lipids.

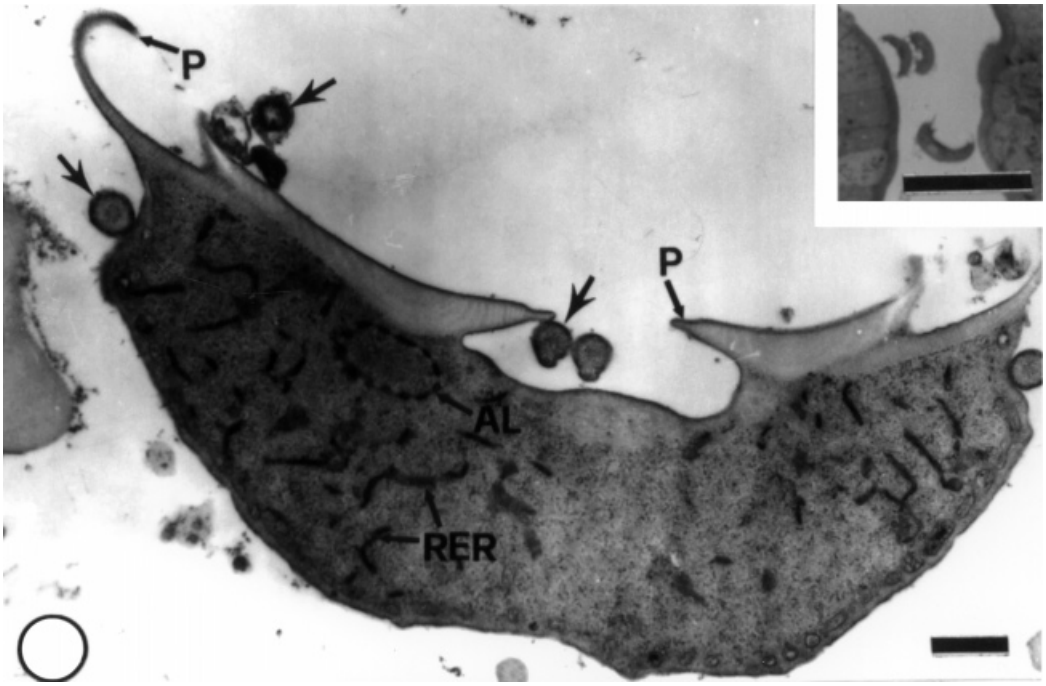

Figure 13. Electron micrograph of the intestinal mucosa of δ-endotoxin-treated group showing an elongated form of cytoplasmic fragments containing several profiles of endoplasmic reticulum (RER), ring-shaped annulate lamellae (AL), clear zones of laterally extended vermiform processes (P), and in association with small rounded structures (arrows) with highly electron dense contour and lightly dense core. Bar = 0.5 μm. Inset: a semithin section of the same area. Bar = 20 μm

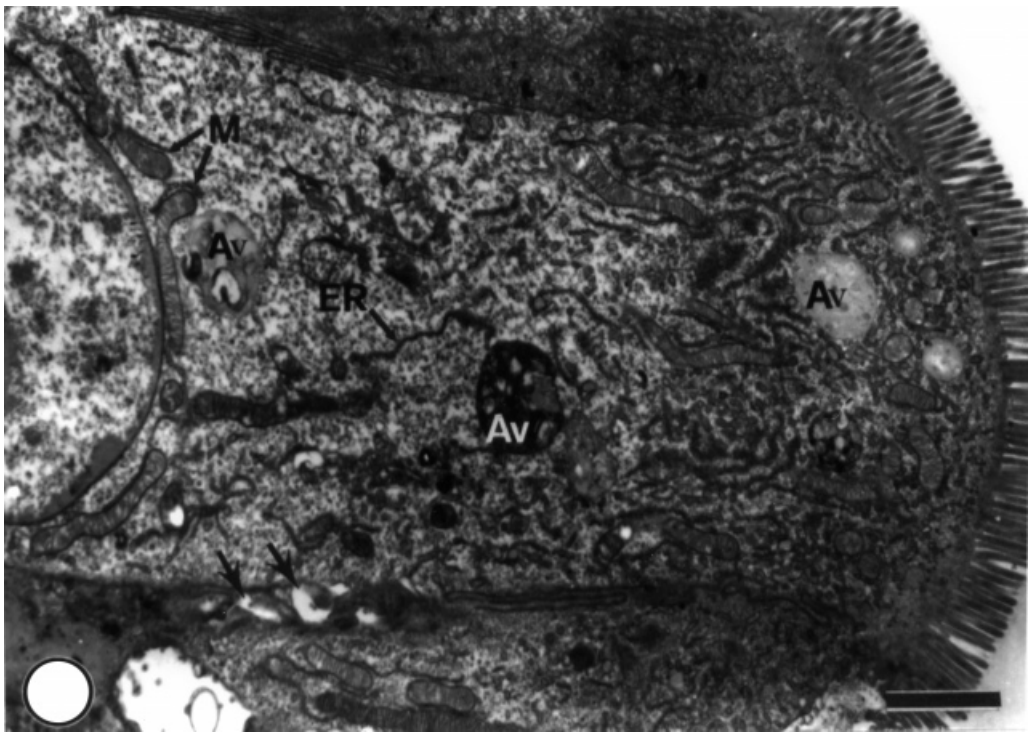

Figure 14. Electron micrograph of the intestinal mucosa of δ-endotoxin-treated group showing detached lateral plasma membranes (arrows), several profiles of endoplasmic reticulum (ER), auotophagic vacuoles (Av), a few mitochondria (M) and a cytoplasmic vacuole. Bar = 2.0 μm

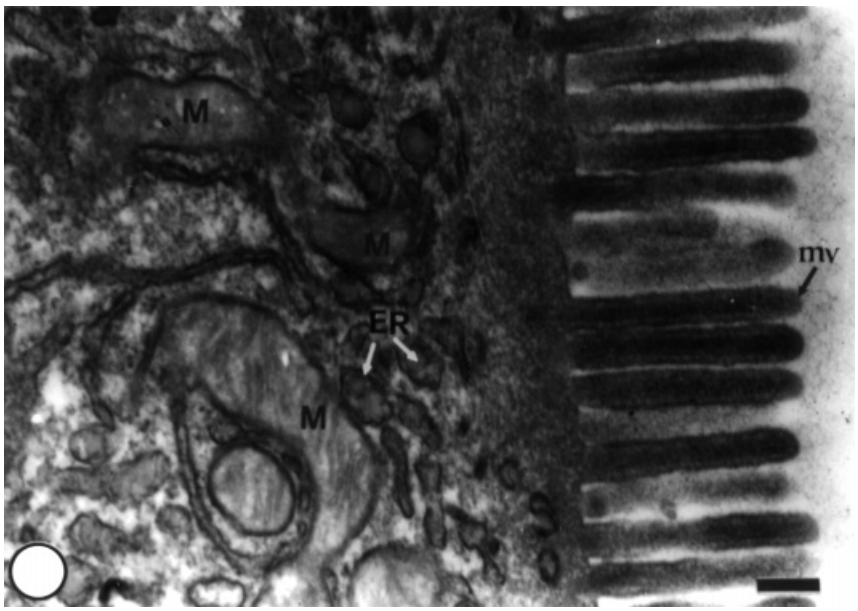

Figure 15. High power electron micrograph of the intestinal mucosa of δ-endotoxin-treated group showing an enterocyte with degenerated forms of mitochondria (M), endoplasmic reticulum (ER) and short microvilli (mv). Bar = 0.2 μm

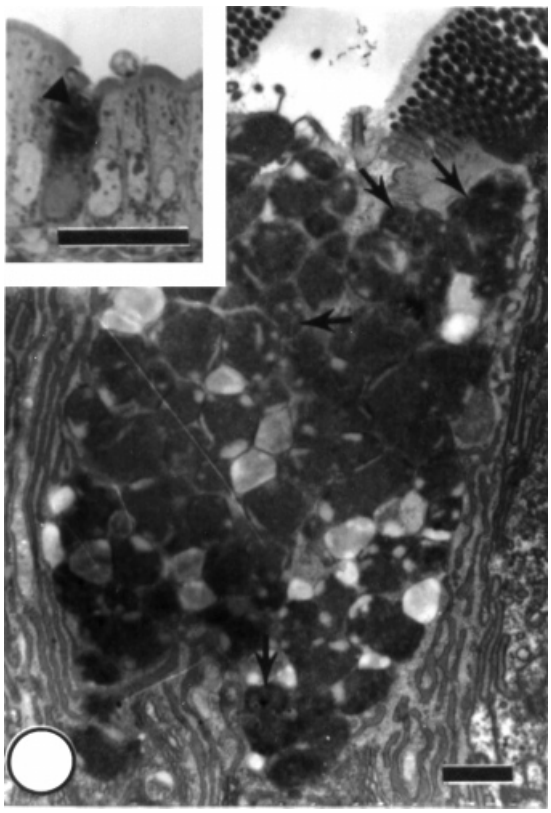

Figure 16. High power electron micrograph of the intestinal mucosa of δ-endotoxin-treated group showing a mucous cell containing several coagulated mucin granules (arrows). Bar = 1.0 μm. Inset: res a mucous cell (arrowhead) in a semithin section of similar area. Bar = 20 μm

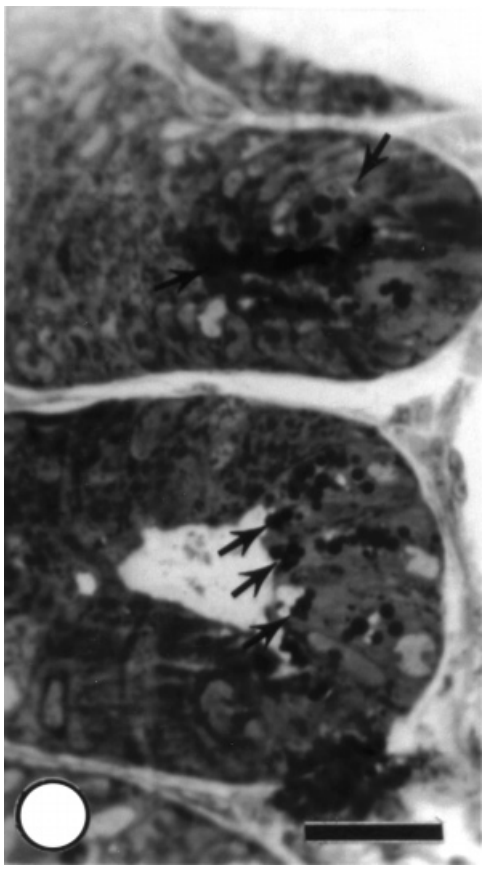

Figure 17. Semithin section of the intestinal mucosa of δ-endotoxin-treated group showing crypts of Lieberkühn with highly activated Paneth cells (arrows). Bar = 20 μm

Figure 18. Scanning electron micrograph of the intestinal mucosa of transgenic potatoes-fed group revealing normal topographic configuration of the enterocytes (asterisks) of the intestinal villi (arrows). Bar = 10 μm

They postulated that the 27 kDa protein was the toxin responsible for cytolytic activity, and acted by binding to the fatty acids phosphatidyl choline and sphingomyelin, among others, as long as these contained unsaturated acyl residues.

In the present investigation, the absence of luminal microvilli in several foci and their association with variable-shaped cytoplasmic fragments in certain other areas may provide a strong evidence of the cytolytic action of the δ-endotoxin of *Bacillus thuringiensis kurstaki* on the intestinal lining epithelium of mice. Some of these fragments contained several profiles of endoplasmic reticulum, as well as ring-shaped annulate lamellae. The presence of annulate lamellae in these cytoplasmic fragments may indicate that they were parts of hyperplastic cells, since several studies revealed the presence of these unique structures in carcinoma cell lines and malignant tumors (Goodlad and Fletcher, 1991; Mirejovsky, 1991; Ueda *et al.*, 1991; Wang *et al.*, 1992; Pettinato *et al.*, 1993). These lamellae are considered to be derived from the outer lamellae of the nuclear membranes or from the intracytoplasmic endoplasmic

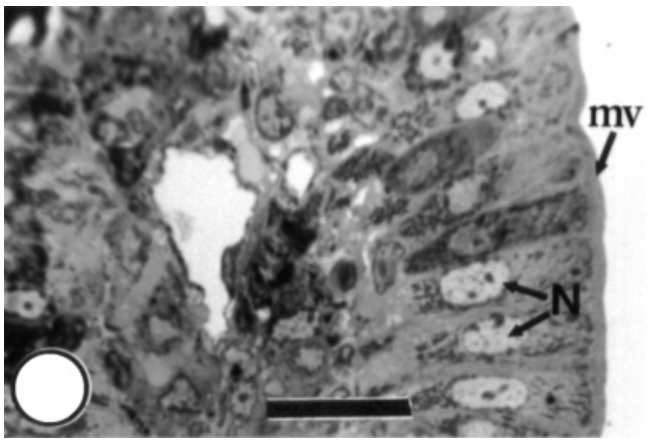

Figure 19. Semithin section of the intestinal mucosa of transgenic potatoes-fed group revealing enterocytes with normal elongated nuclei (N) and normally organized microvilli (mv). Bar = 20 μm

reticulum (Johannessen, 1979). They are mainly found in rapidly proliferating cell systems, since they may have a role in the nucleocytoplasmic exchange of substances necessary for accelerated protein synthesis, especially in hyperplastic cells. In addition, these fragments were associated with much smaller and rounded structures. These small structures were similar to parasporal bodies of the *Bacillus thuringiensis kurstaki* in their highly electron dense contour and lightly dense core, as previously described by several investigators (Insell and Fitz-James, 1985; Lee *et al.*, 1985; Ibarra and Federici, 1986a). Immunological studies showed that δ-endotoxin of *Bacillus thuringiensis* interacts with the microvilli of the midgut epithelial cells of insects (Ravoahangimalala *et al.*, 1993; Aranda *et al.*, 1996).

In the present investigation a few common features, including mitochondria with signs of degeneration and disrupted short microvilli, were recognized in the

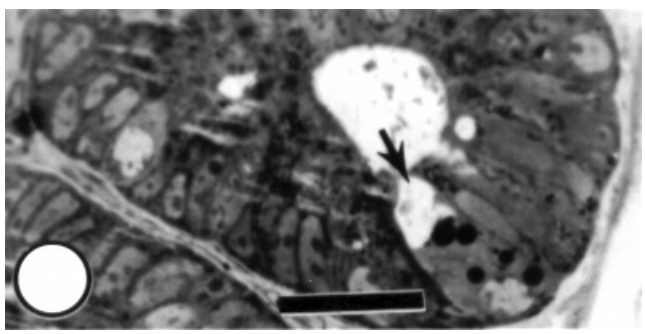

Figure 20. Semithin section of a part of the intestinal mucosa of transgenic potatoes-fed group revealing Paneth cells, with a few secretory granules (arrow), within the crypts of Lieberkühn. Bar = 20 μm

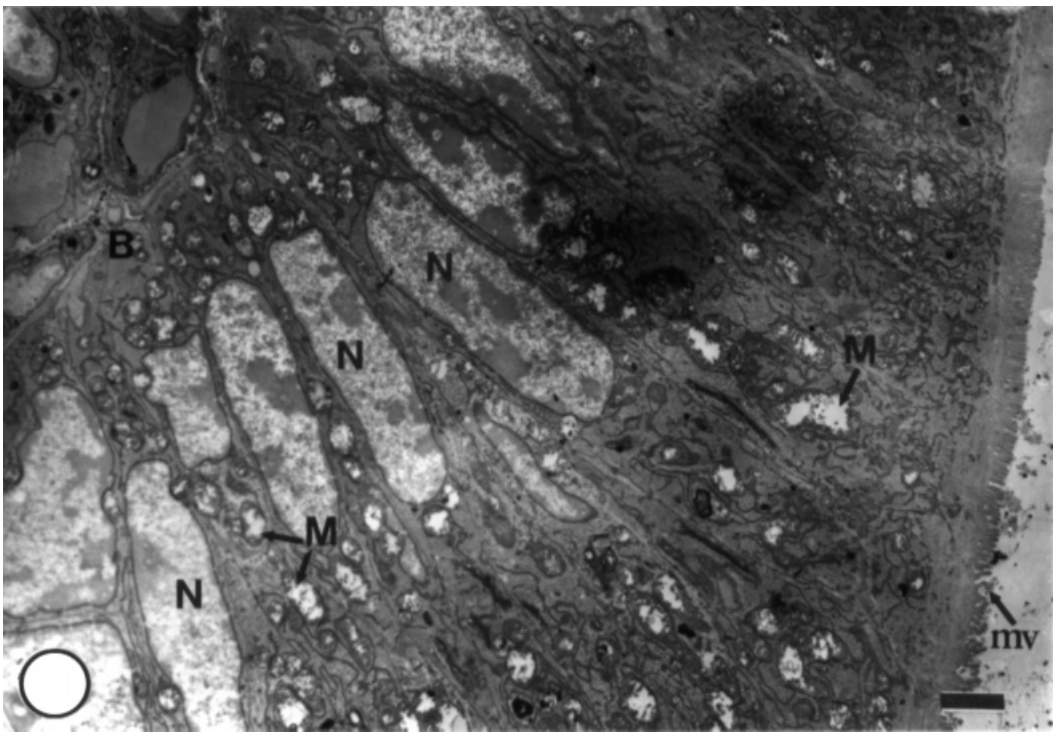

Figure 21. Electron micrograph of the intestinal mucosa of transgenic potatoes-fed group revealing enterocytes with elongated nuclei (N), a relatively intact basal lamina (B) and several dilated mitochondria with short cristae (M). The luminal surface of certain foci possessed disrupted short microvilli (mv). Bar = 2.0 μm

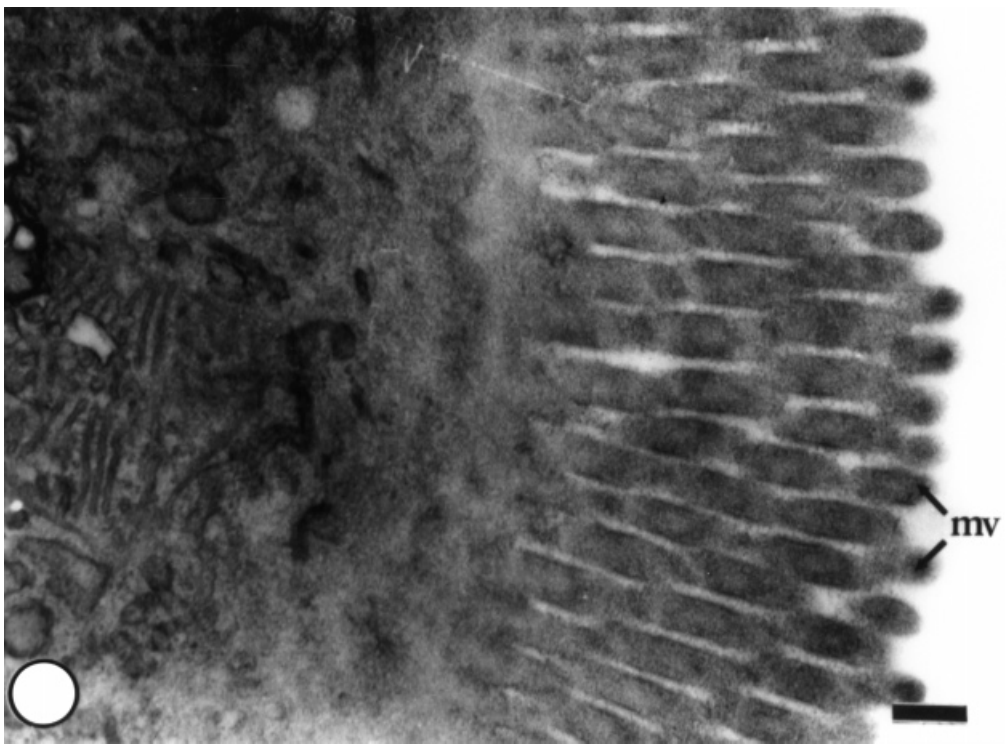

Figure 22. High power electron micrograph of the intestinal mucosa of transgenic potatoes-fed group revealing normally organized microvilli (mv). Bar = 0.2 μm

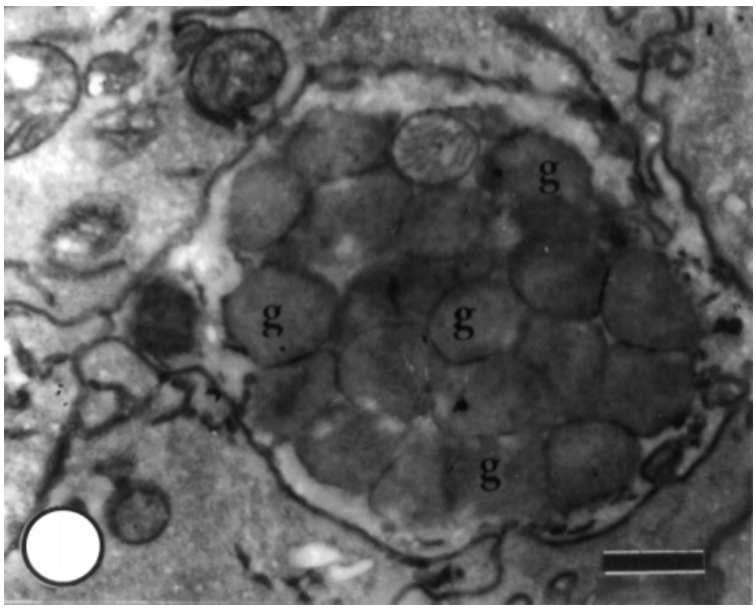

Figure 23. High power electron micrograph of the intestinal mucosa of transgenic potatoes-fed group revealing a mucous gland with homogeneous mucin granules (g). Bar = 0.5 μm

ultrastructure of the intestinal epithelium in both groups of mice fed on δ-endotoxin-treated potatoes and transgenic potatoes. However, in the group of mice fed on the δ-endotoxin-treated potatoes, the Paneth cells of the crypts of Lieberkühn were highly activated and contained a large number of secretory granules. These cells are believed to have an important role in the activation of phagocytes and controlling the bacterial flora of the gut (Ariza *et al.*, 1996; Fawcett, 1997). They contain elevated levels of lysozyme in their large eosinophilic secretory granules, an enzyme capable of digesting bacterial cells walls, and antibacterial peptides called cryptdins (Junqueira *et al.*, 1998). Ouellette (1997) revealed that Paneth cell secretory products seem to contribute both to innate immunity of the crypt lumen and to defining the apical environment of neighboring cells. Wada *et al.* (1993) revealed that the incidence of Paneth cells increases in adenomas and adenocarcinoma, as well as in several other diseased digestive tracts. The antimicrobial polypeptides of the Paneth cell secretory products kill a wide range of organisms, including bacteria, fungi, viruses and tumor cells (Aley *et al.*, 1995).

In conclusion, the present investigation revealed mild changes in the microscopic structure of the different cellular compartments of the ileum of a group of mice fed on transgenic potatoes as compared with another group of mice fed on the δ-endotoxin-treated potatoes, despite the presence of the same type of toxin of *Bacillus thuringiensis* var. *kurstaki* in the transgenic potatoes as a result of gene expression. The appearance of several multinucleated and hypertrophied enterocytes, as well as several associated cytoplasmic fragments with highly recognized annulate lamellae may suggest the possible participation of feeding on the δ-endotoxin-treated potatoes in the hyperplastic development in the mice ileum. Although transgenic crop plants used in food and feed production carry different beneficial transgenes, mostly for resistance to pests, herbicides and diseases (Ondrej and Drobnik, 1997), before releasing for marketing thorough tests and all possible consequences of these new types of heredity and new genetic structures must be evaluated to avoid any potential risks,

ACKNOWLEDGEMENTS

The authors wish to express their appreciation to Dr John C. Herr, Professor of Cell Biology and Director of the Center for Recombinant Gamete Contraceptive Vaccinogens, at the University of Virginia Science Health Center, for providing computer facilities for the finalizing of the present manuscript. Thanks are also due to Dr. Mohamed Salama, Associate Professor of Molecular Biology, at the Department of Entomology, Faculty of Science, Ain Shams University, for providing the transgenic potatoes.

REFERENCES

Aley S, Zimmerman M, Hetsko M, Selsted M, Gillin F (1995). Killing of *Giardia lamblia* by cryptdins and cationic neutrophil peptides. *Infection and Immunity* **62**:5397–5403.

Aranda E, Sanchez J, Peferoen M, Guereca L, Bravo (1996). A Interactions of *Bacillus thuringiensis* crystal proteins with the

midgut epithelial cells of *Spodoptera frugiperda* (Lepidoptera: Noctuidae). *J Invertebr Pathol* **68**:203–212.

Ariza A, Lopez D, Castella E, Munoz C, Zujar M, Mate L (1996). Expression of CD15 in normal and metaplastic Paneth cells of the digestive tract. *J Clin Pathol (London)* **49**:474–477.

Caramori T, Albertini AM, Galizzi A (1991). *In vivo* generation of hybrids between two *Bacillus thuringiensis* insect-toxin-encoding genes. *Gene* **98**:37–44.

Chilcott C, Ellar D (1988). Comparative toxicity of *Bacillus thuringiensis* var. *israelensis* crystal proteins *in vivo* and *in vitro*. *J Gen Microbiol* **134**:2551–2558.

de Barjac H (1989). New facts and trends in bacteriological control of mosquitoes. *Memorias do Instituto Oswaldo Cruz* **84**(suppl 3):101–105.

Fares NH (1996). Histological and fine structural changes in the kidney cortex of mice treated by the carbamate insecticide sevin. *J Egypt Ger Soc Zool* **21**(C):53–85.

Fawcett DW (1997). Bloom and Fawcett: *Concise Histology*. R. P. Jensh, Contributing Editor. Chapman and Hall, Thomson International Publishing, New York, NY, USA.

Goodlad J, Fletcher C (1991). Malignant peripheral nerve sheath tumor with annulate lamellae mimicking pleomorphic malignant fibrous histiocytoma *J Pathol* **164**:23–30.

Ibarra J, Federici B (1986a). Isolation of a relatively nontoxic 65-kilodalton protein inclusion from the parasporal body of *Bacillus thuringiensis* subsp. *Israelensis*. *J Bacteriol* **165**:527–533.

Ibarra J, Federici B (1986b). Parasporal bodies of *Bacillus thuringiensis* subsp. *Morrisoni* (PG-14) and *Bacillus thuringiensis* subsp. *israelensis* are similar in protein composition and toxicity. *FEMS Microbiol Lett* **34**:79–84.

Insell J, Fitz-James P (1985). Composition and toxicity of the inclusion of *Bacillus thuringiensis* subsp. *Israelensis*. *Appl Environ Microbiol* **50**:56–62.

Johannessen J, ed. (1979). *Electron microscopy in Human medicine*, vol. **9**, Urogenital System and Breast. New York: McGraw-Hill International Book Company.

Junqueira L, Carneiro R, Kelley R (1998). Basic Histology, 8th edn. Appleton and Lange, USA.

Lee S, Eckblad W, Bulla L (1985). Diversity of protein inclusion bodies and identification of mosquitocidal protein in *Bacillus thuringiensis* subsp. *Israelensi*. *Biochem Biophys Res Commun* **126**:953–960.

Lüthy P, Ebersold H (1981). *Bacillus thuringiensis* delta endotoxin: histopathology and molecular mode of action. In: Davidson W, ed. *Parthenogenesis of invertebrate microbial diseases*. New Jersey: 235–267.

Mirejovsky P (1991). The ultrastructure of respiratory tract tumors. *Acta Universitatis Carolinae Medica Monographia* **139**:1–25.

Ondrej M, Drobnik M (1997). The safety and usefulness of transgenic plants. *Cas Lek Cesk* **136**:331–336.

Ouellette A (1997). Paneth cells and innate immunity in the crypt microenvironment. *Gastroenterology* **113**:1779–1784.

Pettinato G, Manivel J, Ravetto C T, Gould E, Tuoro A, Jaszcz W, Albores-Saavedra J (1993). Papillary cystic tumor of the pancreas: a linicopathologic study of 20 cases with cytologic, immunohistochemical, ultrastructural, and flow cytometric observations, and a review of the literature. *Am J Clin Pathol* **98**:478–488.

Redway K, Lapage S (1974). Effect of carbohydrates and related compounds on the long-term reservation of freeze-dried bacteria. *Cryobiology* **11**:73–79.

Ravoahangimalala O, Charles J, Schoeller-Raccaud J (1993). Immunological localization of *Bacillus thuringiensis serovar israelensis* toxins in midgut cells of intoxicated *Anopheles gambiae* larvae (Diptera: Culicidae). *Res Microbiol* **144**:271.

Sanchis V, Agaisse H, Chaufaux J, Lereclus D (1996). Construction of new insecticidal *Bacillus thuringiensis* recombinant strains by using the sporulation non-dependent expression system of cryIIIA and a site specific recombination vector. *J Biotechnol* **48**:81–96.

Singsit C, Adang M, Lynch R, Anderson W, Wang A, Cardineau G, Ozias-Akins P (1997). Expression of a *Bacillus thuringiensis* cryIA(c) gene in transgenic peanut plants and its efficacy against lesser cornstalk borer. *Transgenic Res* **6**:169–176.

Thomas W, Ellar D (1983a). *Bacillus thuringiensis* var. *Israelensis* crystal δ-endotoxin: effects on insects and mammalian cells *in vitro* and *vivo*. *J Cell Sci* **60**:181–197.

Thomas W, Ellar D (1983b). Mechanism of action of *Bacillus thuringiensis* var. *Israelensis* insecticidal δ-endotoxin. *FEBS Lett* **154**:362–368.

Travers R, Martin P, Reichelderfer C (1987). Selective process for efficient isolation of soil *Bacillus* spp. *Appl Environ Microbiol* **53**:1263–1266.

Tyrell D, Bulla L, Andrews R, Kramer K, Davidson L, Nordin P (1981). Comparative biochemistry of entomocidal parasporal crystals of selected *Bacillus thuringiensis* strains. *J Bacteriol* **145**:1052–1062.

Ueda N, Nagakawa T, Nakamura A, Ueno K, Miyazaki I, Kurachi M, Konishi I, Hirono T (1991). Clinicopathological studies on solid and cystic tumors of the pancreas. *Gastroenterologia, Joponica* **26**:497–502.

Venable J, Coggeshall R (1965). A simplified lead citrate stain for use in electron microscopy. *J Cell Biol* **25**:407–408.

Wada R, Miwa H, Abe H, Santo R, Kitamura S, Kuwabara N, Suda K, Kondo K, Yamada S (1993). Incidence of Paneth cells in minute tubular adenomas and adenocarcinomas of the large bowel. *Acta Pathol Jap* **42**:579–584.

Wang N, Liu C, Emond J, Tsao M (1992). Annulate lamellae in a large cell lung carcinoma cell line with high expression of tyrosine kinase receptor and proto-oncogenes. *Ultrastructural Pathol* **16**:439–449.

Wu D, Chang F (1985). Synergism in mosquitocidal activity of 26 and 65 kDa proteins of *Bacillus thuringiensis* subsp. *Israelensis* crystal. *FEBS Lett* **190**:232–236.

